Multiparticle He Fragmentation of ^{22}Ne, ^{24}Mg and ^{28}Si in Emulsion at 4.1- 4.5 A GeV/c.

N. P. Andreeva[a], D. A. Artemenkov[b], V. Bradnova[b], M. M. Chernyavsky[c], A. Sh. Gaitinov[a], N. A. Kachalova[b], S. P. Kharlamov[c], A. D. Kovalenko[b], M. Haiduc[d], S. G. Gerasimov[c], L. A. Goncharova[c], V. G. Larionova[c,†] A. I. Malakhov[b], A. A. Moiseenko[e], G. I. Orlova[c], N. G. Peresadko[c], N. G. Polukhina[c], P. A. Rukoyatkin[b], V. V. Rusakova[b], V. R. Sarkisyan[e], T. V. Shchedrina[b], E. Stan[b,d], R. Stanoeva[b,f], I. Tsakov[f], S. Vokál[b,g], A. Vokálová[b], P. I. Zarubin[b] and I. G. Zarubina[b]

a) Institute for Physics and Technology, Almaty, Republic of Kazakhstan
b) Joint Insitute for Nuclear Research, Dubna, Russia
c) Lebedev Institute of Physics, Russian Academy of Sciences, Moscow, Russia
d) Institute of Space Sciences, Bucharest-Mauguerele, Romania
e) Yerevan Physics Institute, Yerevan, Armenia
f) Institute for Nuclear Research and Nuclear Energy, Sofia, Bulgaria
g) P. J. Šafárik University, Košice, Slovak Republic

† *deceased*

Abstract

Characteristics of projectile He fragments from collision of α conjugate nuclei ^{22}Ne, ^{24}Mg and ^{28}Si in emulsion at 4.1- 4.5 A GeV/c have been studies. Only the extra peripheral collisions with more than two He fragments have been used for the analysis. Dependence of the properties of He fragments on their number in the collision and projectile atomic number have been investigated. The distributions of effective masses of two and three He fragments are presented.

1. Introduction

The fragmentation of the relativistic α conjugate nuclei ^{22}Ne, ^{24}Mg and ^{28}Si leading to many α particle final state is aim of this research.

Extra peripheral nuclear interactions are used for analyzes. Extra peripheral interactions have place at minimal excitation of colliding nuclei and are the most resulted for clustering investigation. Extra peripheral nuclear interactions have been selected using criterion: the sum charge of the projectile fragments in the forward narrow cone has to be equal to that of projectile one.

The motivation for the nuclear α fragmentation study is directly connected with such problems as the model of the cluster-like nuclear structure, the nucleosynthesis in the Universe and the prediction for the existence of strongly deformed cluster configurations in light α particle nuclei.

2. Experiment

The experimental results have been obtained using nuclear emulsion method. The stacks of NIKFI BR-2 nuclear photoemulsions have been irradiated horizontally by ^{22}Ne, ^{24}Mg and ^{28}Si at 4.1- 4.5 A GeV/c at the Synchrophasotron of JINR, Dubna. The stacks consisted of a few tens pellicles having dimensions of 20 cm $\times$ 10 cm $\times$ 600 μm. "Along-the-track"double scanning was used to locate interaction in emulsion stacks

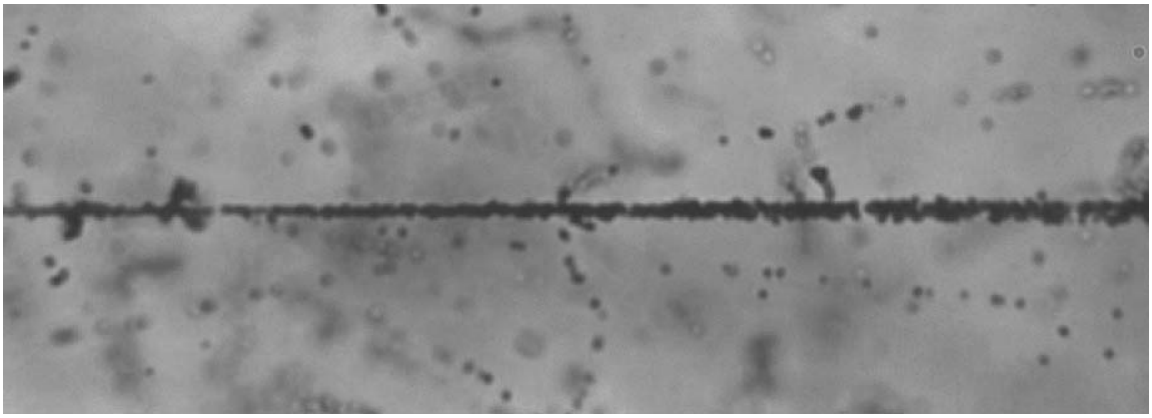

Figure 1: Peripheral interaction of a 2.1 A GeV ^{14}N nucleus in a nuclear track emulsion ("white"star). The interaction vertex and nuclear fragment tracks are seen in a narrow angular cone on the upper and middle microphotographs. Following the direction of the fragment jet, it is possible to distinguish 1 singly and 3 doubly charged fragments (bottom microphotograph).

and to have minimum bias data set. The sensitivity of emulsion (minimal ionization) was 30-35 grains per length of 100 μm for singly charged relativistic particles.

The photoemulsion method allows measuring with higher accuracy and a bigger acceptance that most of the other experiments:

• Multiplicities of any charged particles: produced particles (N_s) with $\beta \geq 0.99$, projectile fragments (N_{fr}) with $\beta \approx 0.99$ and target fragments (N_h) with $\beta < 0.7$;

• Angles of particles with the resolution of $\Delta(\eta)$ =0.01-0.02 rapidity units in the central region, pseudo-rapidity is given by $\eta = -ln(tan(\theta/2))$ and θ is the emission angle with respect to the beam direction;

• Charges of projectile fragments (Z_{fr}) using its gap-length distributions and/or δ-electron densities;

• Momentum of relativistic particles with emission angles $\leq 5^\circ$ using multiple scattering measurements.

However, the problems of the photoemulsion method are rather limited statistics and nonhomogeneous composition.

3. The statistics

It has been used for the analysis only the collisions:

• With more than two projectile He fragments - $N_{He} \geq 3$ and

• Extra peripheral ones with the sum charge in the forward narrow cone been approximately equal to that of projectile one - $\sum Z_{fr} = Z_0 \pm 1$, where Z_0 is projectile charge.

Fraction of such collisions in minimum bias data set is about 10-15%.

In Fig.1 one of such collision is shown. The collision of ^{28}Si at 4.5 A GeV/c has six projectile He fragment, one projectile fragment with Z=1 in narrow forward cone ($\theta \leq 2.5^\circ$) and two shower particles with big angles.

Table 1 presents the used statistic of collisions selected according criteria mentioned above. To increase statistic of seldom collisions with $N_{He} \geq 3$ the additional "area

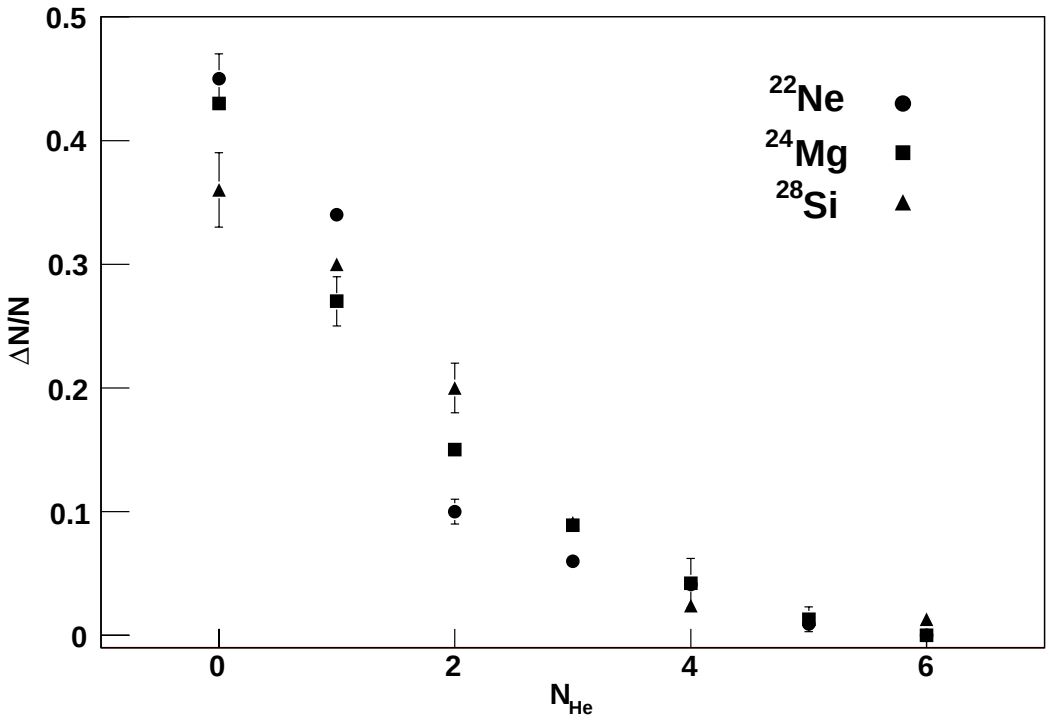

Figure 2: Multiplicity distributions of He fragments for ^{22}Ne, ^{24}Mg and ^{28}Si interactions.

Table 1: The statistic of collisions has been used for analyses.

A_0	P_0, GeV/c	N_{He}=3	N_{He}=4	N_{He}=5	N_{He}=6
^{22}Ne	4.1	238	79	10	0
^{24}Mg	4.5	28	45	8	1
^{28}Si	4.5	107	40	21	13

scanning"have been done, so it is not minimum bias data set in table 1.

4. Results

4.1. The multiplicities of He fragments

The multiplicity distributions of He fragments are shown in Fig.2, there was used the "along-the-track"located collisions only. The fraction of collision with number of projectile He fragments more then three ($N_{He} \geq 3$) increases slowly with increasing of projectile mass: 0.11±0.01, 0.14±0.03 and 0.14±0.02 for ^{22}Ne, ^{24}Mg and ^{28}Si interactions respectively.

Integral multiplicity distribution of He fragments may be fitted by a line with a break at N_{He}=2, that one can see in Fig.3.

Dependences of average number of projectile fragments with $Z_{fr} = 2$ and $Z_{fr} \geq 3$ on the projectile charge Z_0 are shown in Fig.4. One can see that in the region under investigation average number of He fragments increases with increasing of projectile charge as N_{He}=0.28+0.07Z_0, at the same time average number of projectile fragments with $Z_{fr} \geq 3$ decreases slowly as $N_{Z\geq 3}$= 1.11-0.02Z_0. It means that increasing of projectile

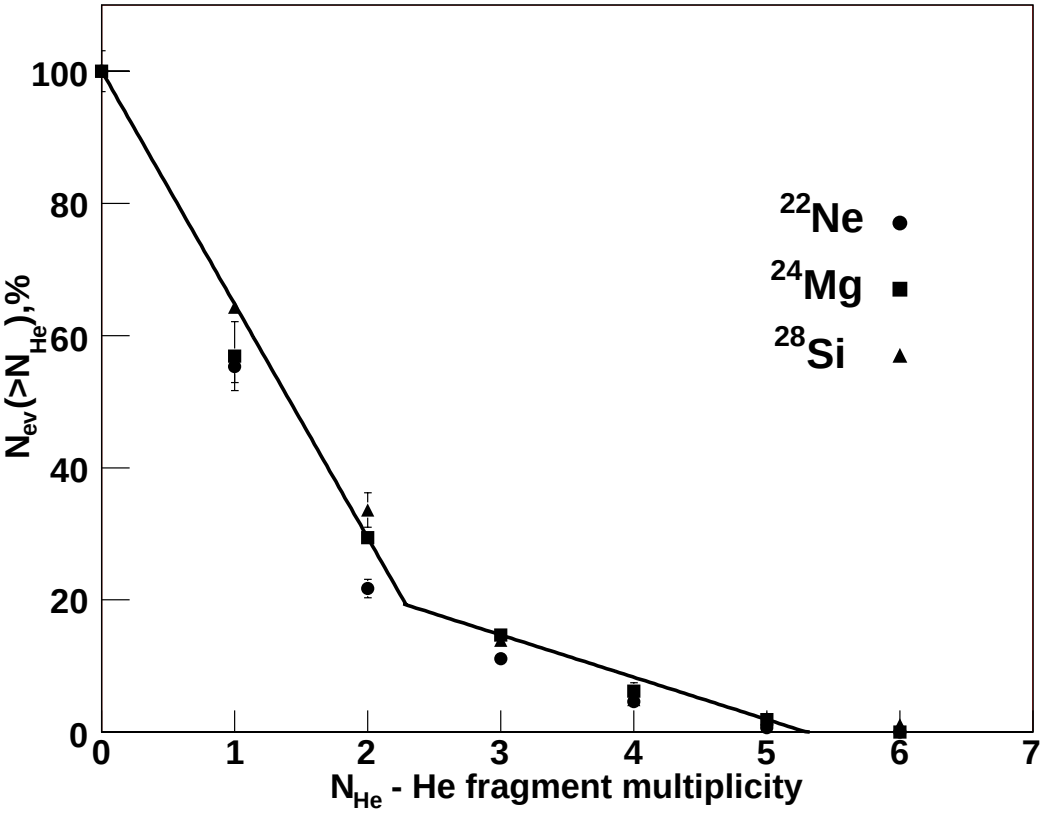

Figure 3: Integral multiplicity distribution of He fragments for ^{22}Ne, ^{24}Mg and ^{28}Si interactions. Fit by sum of two lines is done for ^{22}Ne interactions.

fragments number with increasing of projectile charge is due to number of fragments with charges 1 and 2 only.

4.2. The angles of He fragments

Nearly all projectile fragments with $Z_{fr} \geq 2$ have small emission angles and can be well separated from other particles (see Fig.1.). Projectile fragments with $Z_{fr} \geq 2$ are emitted mostly within the fragmentation cone defined by a critical angle θ_b, where $\sin(\theta_b) = 0.2(\mathrm{GeV/c})/P_0$; for example $\theta_b = 2.55^\circ$ at $P_0 = 4.5$ A GeV/c.

An example of angle distributions of He fragments is shown in Fig.5. In Fig.5 (left) one can see angle distributions for different channels of ^{22}Ne collisions with 3, 4 and 5 He fragments in final state. In Fig.6 it is shown dependences of average emission angles of He fragments on number of He fragments in collision. In Fig.5 (left) and 6 one can see that emission angles of He fragments decrease with increasing of He fragment number in collision. This decreasing may be explained if to admit that He fragments often are result of decays heavier intermediate fragments (Be, C and O). The indirect He fragments have tendencies to save angles of parents, but the more is mass of parent fragment the less is angle they have. If number of such indirect He fragments proportional to the number of He fragments in final state it have to be effect we explain.

In Fig.5 (right) it is shown angle distributions for sum of channels with $N_{He} \geq 3$ of ^{22}Ne, ^{24}Mg and ^{28}Si collision; in Fig.7 the same distributions are shown in integral form. From Fig.5 (right) and Fig.7 one cam conclude that there is not dependence of He fragment angle distributions from projectile mass in the region under investigation.

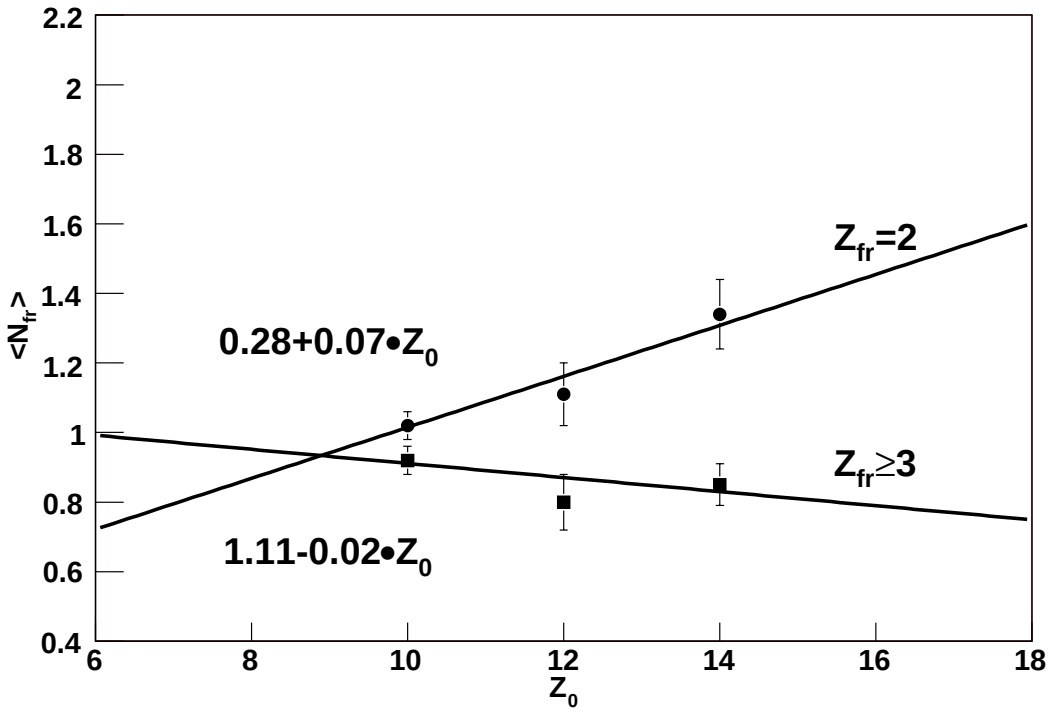

Figure 4: Dependences of average number of projectile fragments with Z_{fr}= 2 and Z_{fr} ≥3 on the projectile charge Z_0.

Integral angular spectrum of He fragments may be fitted by a line (see Fig.7).

4.3 The transverse momentum of He fragments

Transverse momentum of He fragment was calculated by formula $P\perp=4\cdot P_0\sin(\theta)$. Integral $P\perp^2$ distributions of He fragments are shown in Fig.8. One can see that integral $P\perp^2$ distributions of He fragments may be fitted by a line with a break at $P\perp^2 \approx 0.2$ $(GeV/c)^2$. One of the reasons of the break may be admixture of ^{3}He fragments - ^{3}He fragments have in average bigger angles than ^{4}He. The other reason may be existence of two (or more then one) different sources of He fragment formation.

4.4 Distributions of the excitation energy of He fragments

The reconstructed excitation energy spectra for decay ^{8}Be→2He (Fig.9) and for decay ^{12}C→3He (Fig.10) with respect to the ground state of the nuclei ^{8}Be and ^{12}C have been analyzed.

In Fig.9 the excitation energy spectra for decay ^{8}Be→2He are shown for ^{22}Ne collisions with different number of He fragments in final state (a) and for ^{22}Ne, ^{24}Mg and ^{28}Si collisions with N_{He} ≥3 in final state (b). One can see that first five excited levels (E_x ≥15 MeV) are mostly responsible for ^{8}Be→2He decays in our experiment - ≥80% events. Big level width doesnt aloud to separate excited levels in details. It is possible to note that there is no principle difference in form of the excitation energy spectra for collisions with different number of He fragment (Fig.9a) in final state from one side and for ^{22}Ne, ^{24}Mg and ^{28}Si collisions (Fig.9b) from other.

In Fig.10 the excitation energy spectra for decay ^{12}C→3He are shown for ^{28}Si collisions with different number of He fragments in final state (a) and for ^{22}Ne, ^{24}Mg and ^{28}Si collisions with N_{He} ≥3 in final state (b). The excitation energy spectrum structure

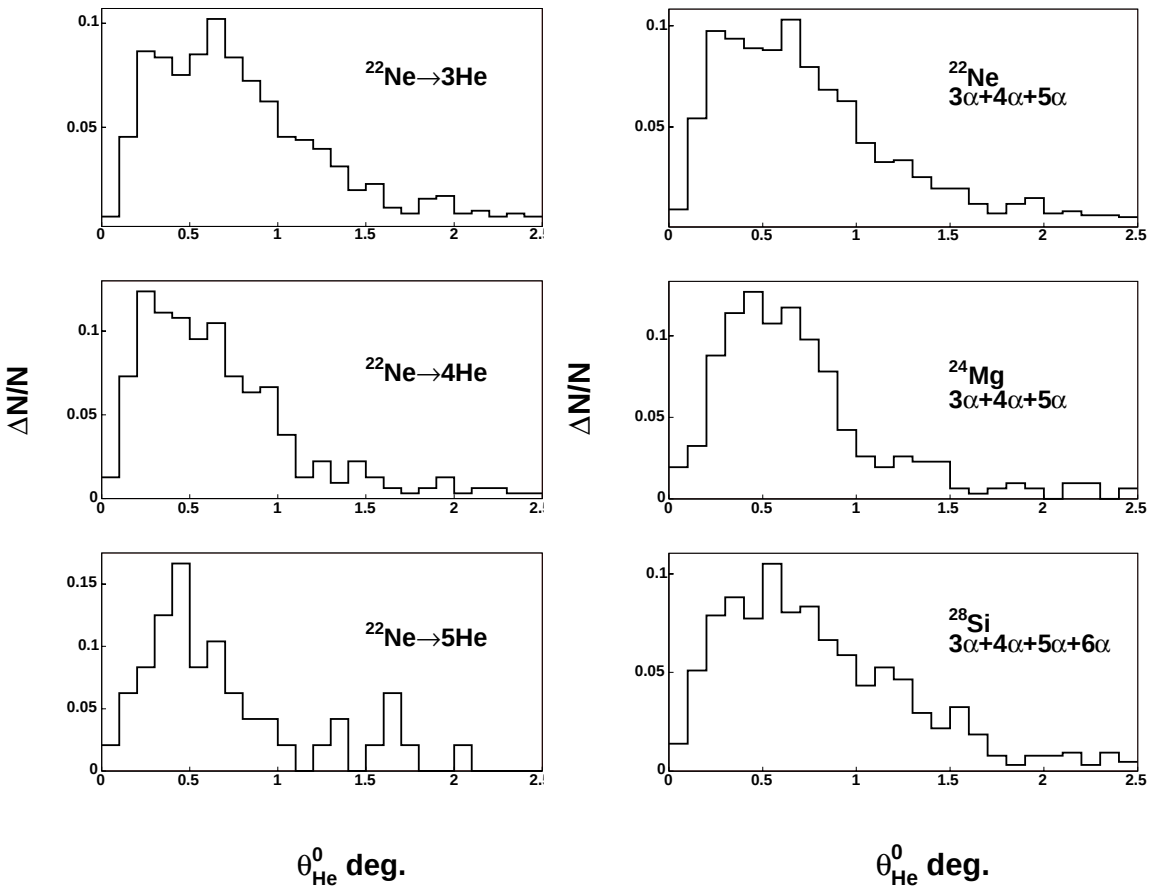

Figure 5: Angle distributions of He fragments: for different channels of ^{22}Ne collisions with 3, 4 and 5 He fragments in final state (left) and for sum of channels with $N_{He} \geq 3$ of ^{22}Ne, ^{24}Mg and ^{28}Si collisions (right).

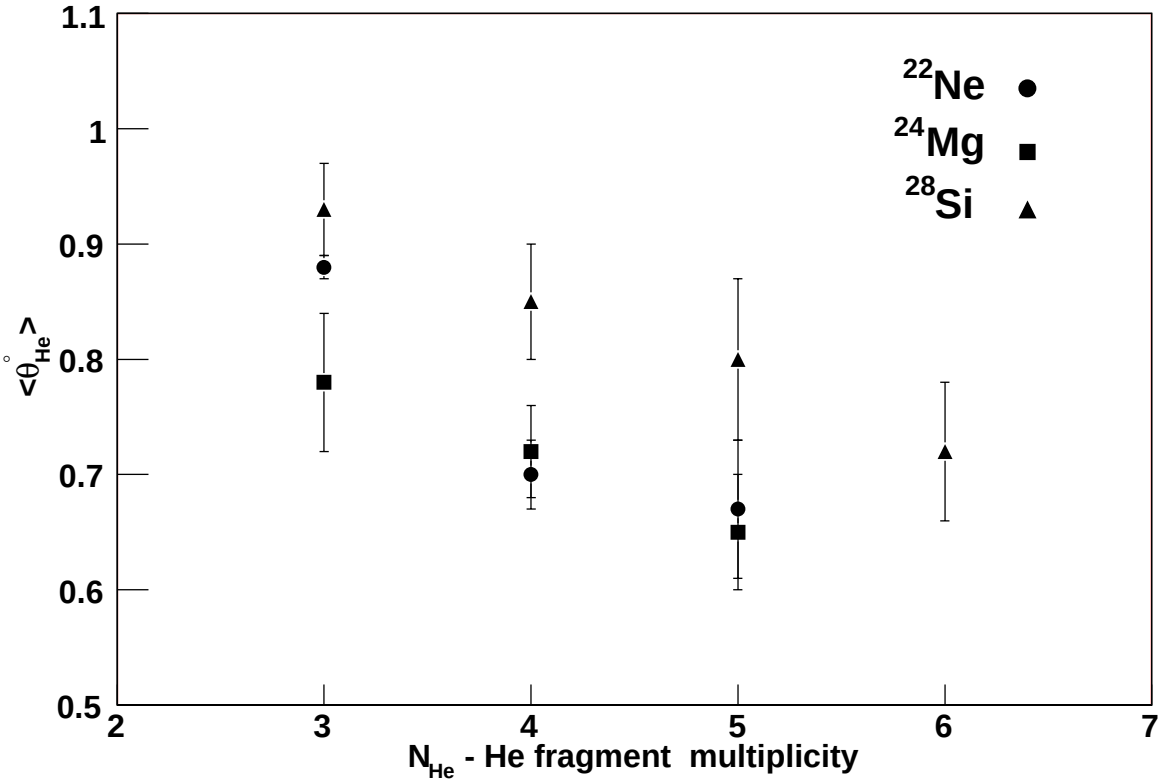

Figure 6: Dependence of average emission angles of He fragments on number of He fragments in collision for ^{22}Ne, ^{24}Mg and ^{28}Si interactions.

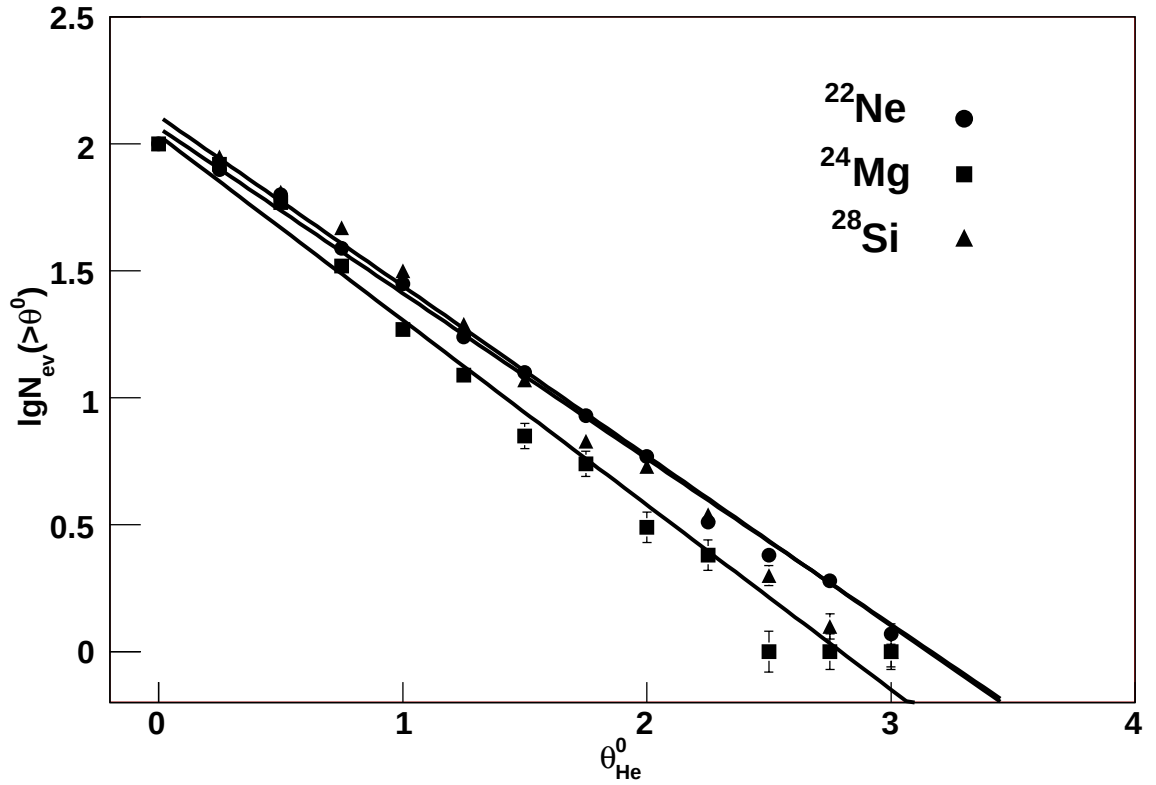

Figure 7: Integral angular spectrum of He fragments from ^{22}Ne, ^{24}Mg and ^{28}Si interactions for sum of channels with $N_{He} \geq 3$.

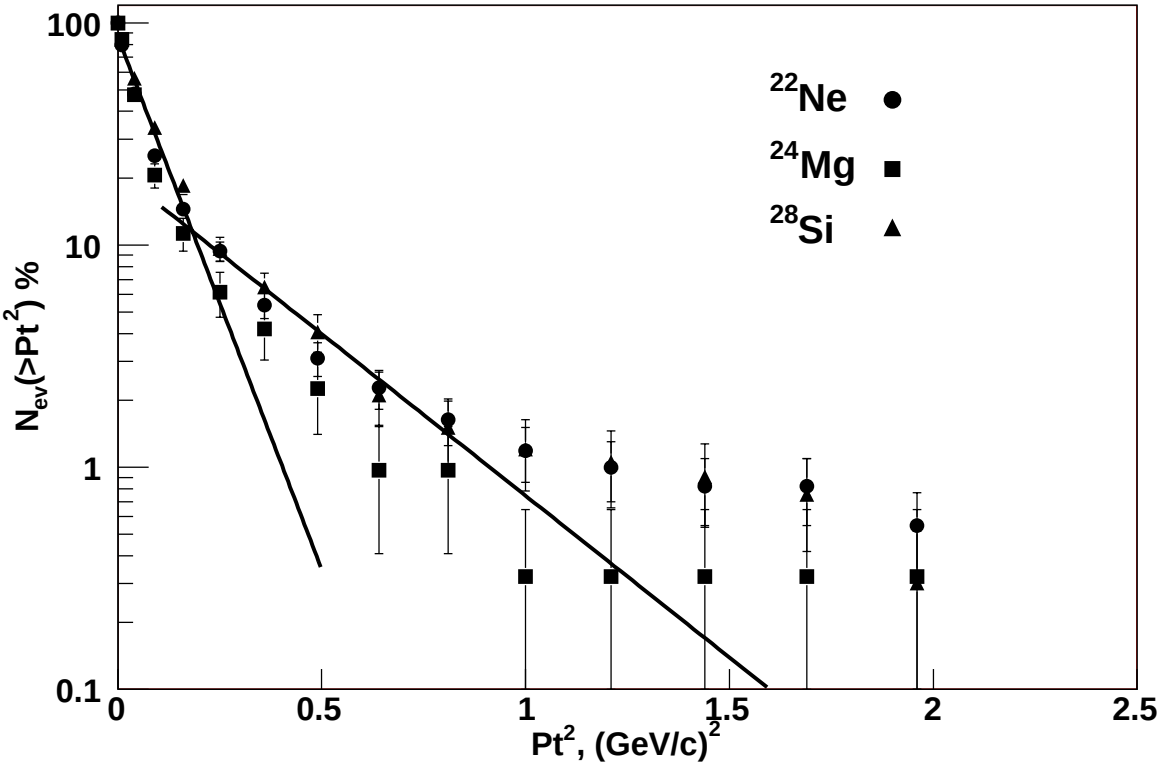

Figure 8: Integral P$\perp^2$ distributions of He fragments from ^{22}Ne, ^{24}Mg and ^{28}Si interactions for sum of channels with $N_{He} \geq 3$.

one can see for channels with 3, 4, 5 and 6 He fragments separately (Fig.10a) disappears in case of spectra for sum of all channels $N_{He} \geq 3$ (Fig.10b). In all cases maximum of excitation energy spectra are in the region $E_x \approx$10-15 MeV. It is possible to note that with increasing of projectile mass the excitation energy spectrum shifts to the bigger meanings; for example, in the region $E_x \geq$15 MeV there are 53, 60 and 66% of events for ^{22}Ne, ^{24}Mg and ^{28}Si collisions, correspondently (Fig.10b).

5. Conclusions

Projectile He fragments from extra peripheral ^{22}Ne, ^{24}Mg and ^{28}Si collisions with $N_{He} \geq 3$ in final state have the next properties:

Integral multiplicity distribution of He fragments may be fitted by a line with a break at N_{He}=2.

In the region under investigation average number of He fragments increases with increasing of projectile charge Z_0 as N_{He}=0.28+0.07·Z_0, average number of projectile fragments with $Z_{fr} \geq 3$ decreases slowly as $N_{Z\geq 3}$ = 1.11-0.02·Z_0;

Average emission angle of He fragments decrease with increasing of He fragment number in collision.

Integral angular spectrum of He fragments may be fitted by a line.

Integral P$\perp^2$ spectrum of He fragments may be fitted by a line with a break at P$\perp^2 \approx$0.2 (GeV/c)^2.

For ^{8}Be→2He decays in the excitation energy region E_x <15 MeV there are more then 80% events.

For ^{12}C→3He decays maximum of excitation energy spectra is in the region $E_x \approx$10-15 MeV.

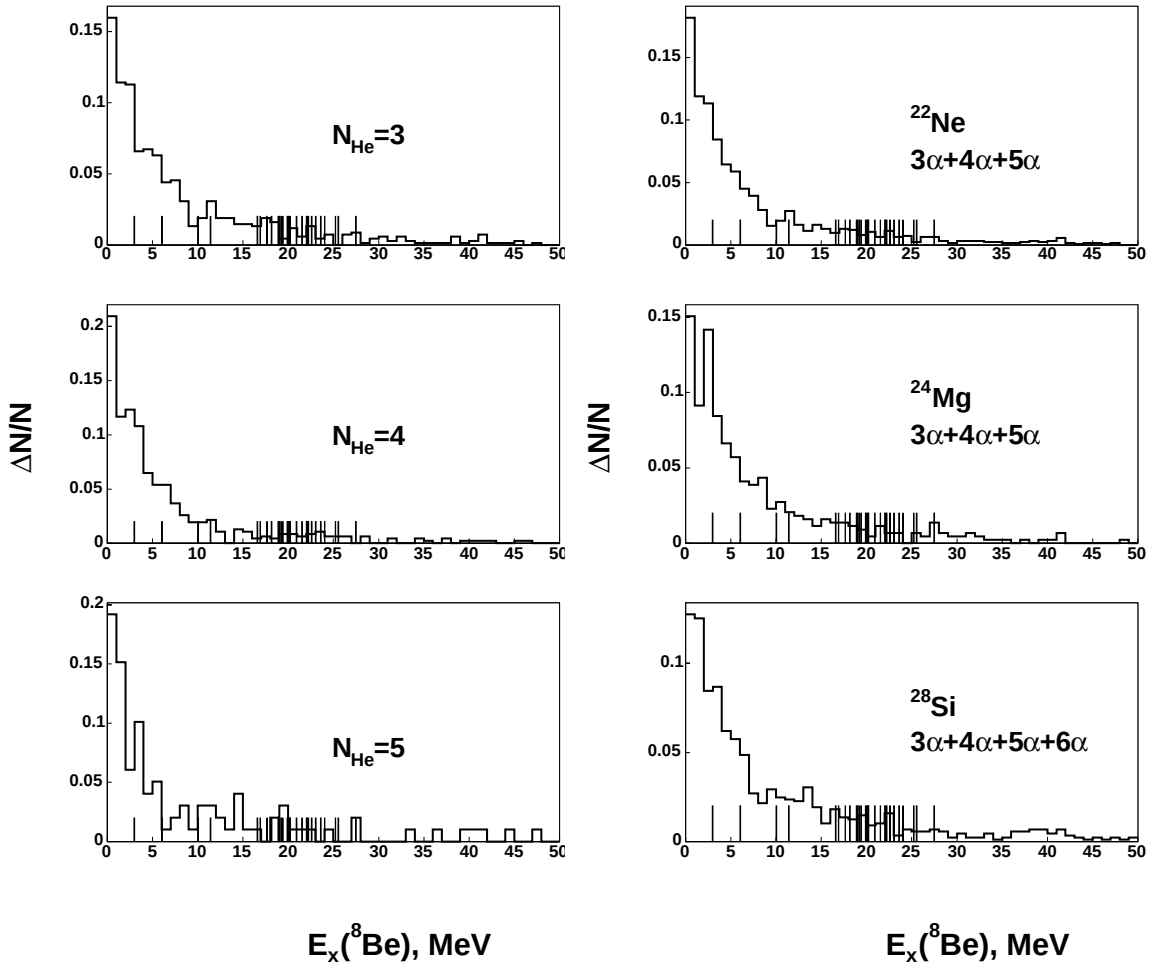

Figure 9: Excitation energy spectra for decay ^{8}Be→2He: a) For ^{22}Ne collisions with different number of He fragments; b) For ^{22}Ne, ^{24}Mg and ^{28}Si collisions with $N_{He} \geq 3$ in final state. Shot lines on the E_x axis are excitation levels of ^{8}Be.

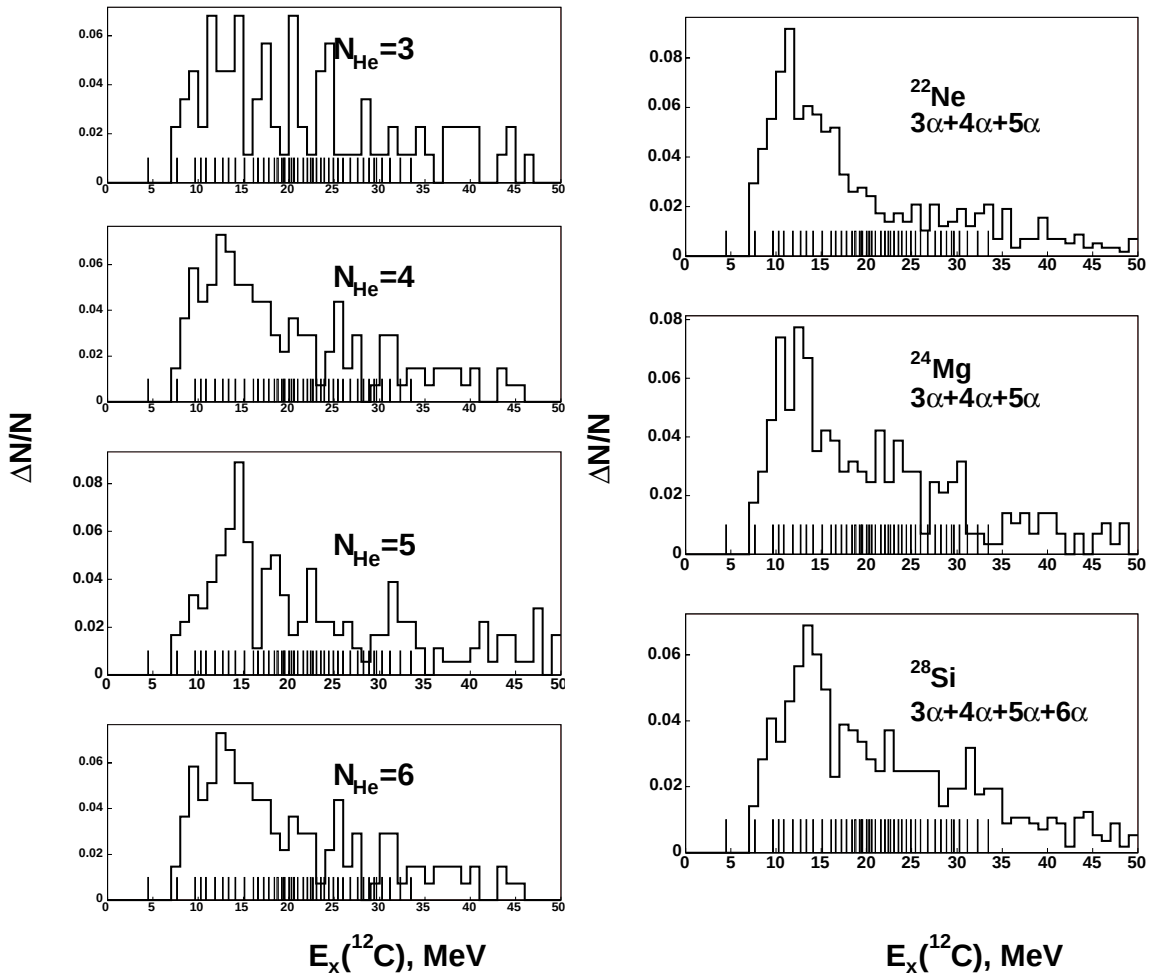

Figure 10: Excitation energy spectra for decay ^{12}C→3He: a) For ^{28}Si collisions with different number of He fragments; b) For ^{22}Ne, ^{24}Mg and ^{28}Si collisions with $N_{He} \geq 3$ in final state. Shot lines on the E_x axis are excitation levels of ^{12}C.

For ^{12}C→3He decays the excitation energy spectrum shifts to the bigger meanings with increasing of projectile mass; for example, in the region $E_x \geq 15$ MeV there are 53, 60 and 66% of events for ^{22}Ne, ^{24}Mg and ^{28}Si collisions, correspondently.

Acknowledgments

The work was supported by the Russian Foundation for Basic Research (Grants nos. 96-1596423, 02-02-164-12a, 03-02-16134, 03-02-17079, 04-02-16593, 04-02-17151), the Agency for Science of the Ministry for Education of the Slovak Republic and the Slovak Academy of Sciences (Grants VEGA 1/9036/02 and 1/2007/05) and Grants from the JINR Plenipotentiaries of Bulgaria, Czech Republic, Slovak Republic, and Romania during years 2002-5.